JCTC Journal of Chemical Theory and Computation

Potential Energy Landscape of the Electronic States of the GFP Chromophore in Different Protonation Forms: Electronic Transition Energies and Conical Intersections

I. V. Polyakov,*,† B. L. Grigorenko,† E. M. Epifanovsky,‡ A. I. Krylov,‡ and A. V. Nemukhin†,§

Department of Chemistry, M.V. Lomonosov Moscow State University, Moscow 119991, Russian Federation, Department of Chemistry, University of Southern California, Los Angeles, California 90089, and Institute of Biochemical Physics, Russian Academy of Sciences, Moscow 119334, Russian Federation

Received May 3, 2010

Abstract: We present the results of quantum chemical calculations of the transition energies and conical intersection points for the two lowest singlet electronic states of the green fluorescent protein chromophore, 4′-hydroxybenzylidene-2,3-dimethylimidazolinone, in the vicinity of its cis conformation in the gas phase. Four protonation states of the chromophore, i.e., anionic, neutral, cationic, and zwitterionic, were considered. Energy differences were computed by the perturbatively corrected complete active space self-consistent field (CASSCF)-based approaches at the corresponding potential energy minima optimized by density functional theory and CASSCF (for the ground and excited states, respectively). We also report the EOM-CCSD and SOS-CIS(D) results for the excitation energies. The minimum energy S_0/S_1 conical intersection points were located using analytic state-specific CASSCF gradients. The results reproduce essential features of previous *ab initio* calculations of the anionic form of the chromophore and provide an extension for the neutral, cationic, and zwitterionic forms, which are important in the protein environment. The S_1 PES of the anion is fairly flat, and the barrier separating the planar bright conformation from the dark twisted one as well as the conical intersection point with the S_0 surface is very small (less than 2 kcal/mol). On the cationic surface, the barrier is considerably higher (∼13 kcal/mol). The PES of the S_1 state of the zwitterionic form does not have a planar minimum in the Franck−Condon region. The S_1 surface of the neutral form possesses a bright planar minimum; the energy barrier of about 9 kcal/mol separates it from the dark twisted conformation as well as from the conical intersection point leading to the cis−trans chromophore isomerization.

Introduction

The fascinating photochemical properties of the green fluorescent protein (GFP), which is employed in many areas of biotechnology and medicine as a biomarker in living cells,[1−3] have inspired numerous experimental and theoretical studies.[4−6] An important practical goal is to formulate concrete suggestions to guide the design of novel biomarkers by modifying either the structure of the chromophore or its immediate environment (specific amino acid residues) in fluorescent proteins of the GFP series. This requires a mechanistic understanding of transformations occurring with the chromophore upon photoexcitation, which includes characterization of absorption and emission bands in optical spectra as well as evolution of the system in the excited electronic states in various environments. From the theoreti-

* Corresponding author e-mail: polyakoviv@gmail.com.
† M.V. Lomonosov Moscow State University.
‡ University of Southern California.
§ Russian Academy of Sciences.

10.1021/ct100227k
Published on Web 07/20/2010

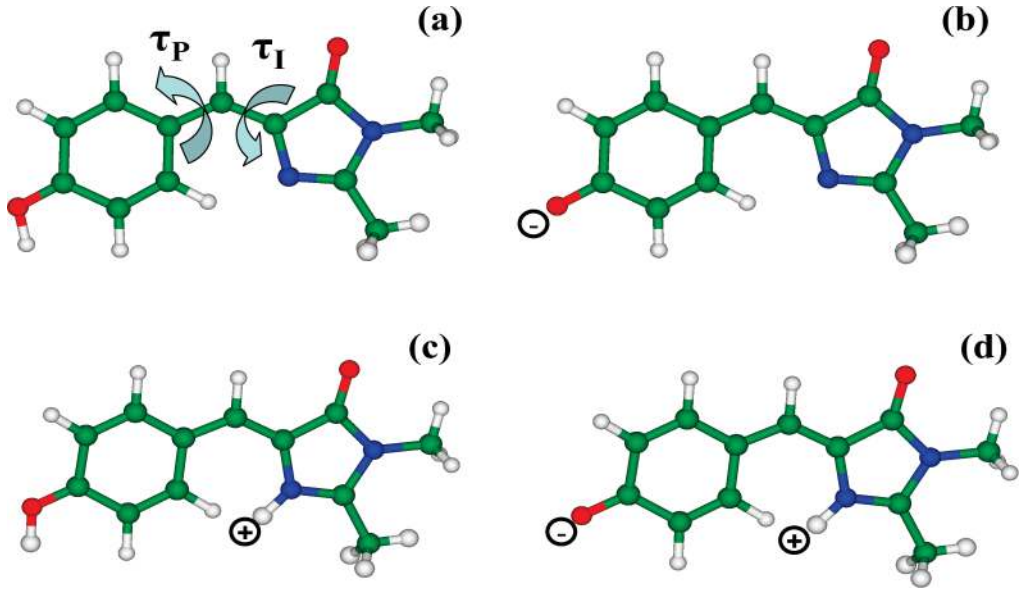

Figure 1. Protonation forms of the GFP chromophore, HBDI, in the cis conformation: (a) neutral, (b) anionic, (c) cationic, and (d) zwitterionic. Here and below, the carbon atoms are colored in green, nitrogen in blue, and oxygen in red. The definition of the twisting angles around the phenolate (P) and imidazolidinone (I) bridge bonds, τ_P and τ_I, is shown in panel a.

cal perspective, the characterization of denatured (isolated) chromophores is the first step toward understanding their photochemical properties in realistic environments. Modeling isolated species involves calculations of the properties of the chromophores in the gas phase and in solution using quantum chemistry methods.

The experimental studies of the GFP-type chromophores in the gas phase[7−11] provide important information on the structure and spectra of these species. The works of Andersen et al.[7−10] characterized the absorption bands corresponding to the S_0-S_1 vertical excitation by the photodestruction spectroscopy of mass-selected ions injected into an electrostatic ion storage ring. The band maxima for the anionic and cationic forms (Figure 1b and c) of the GFP chromophore, 4′-hydroxybenzylidene-2,3-dimethylimidazolinone (HBDI) were reported at 479 and 406 nm (2.59 and 3.05 eV), respectively. To mimic the neutral species (Figure 1a), the so-called, "neutral+" analogs were used. The earlier study reported the value 415 nm (2.99 eV),[9] while in the later paper the authors reported a revised value of 370 nm (3.35 eV).[10] Forbes and Jockusch studied the gaseous HBDI anion in the ion trap measuring laser induced fluorescence and photoactivation action spectra.[11] No fluorescence was detected in these experiments, and electron detachment and fragmentation were found to be the primary modes of ion deactivation.

The absence of fluorescence in the gas phase is consistent with the solution results—the fluorescence quantum yield of HBDI in solution drops by more than 3 orders of magnitude relative to wild-type GFP. This is attributed to ultrafast (∼0.5−2 ps) internal conversion (IC) of the denaturated chromophore to the ground state, in contrast to the nanosecond lifetime of the excited state in the protein environment. The mechanism of IC is still not clear. Solution studies showed that there is no correlation with solvent viscosity (which can be modified by either using different solvents or by varying the temperature), which can only be explained by volume-conserving and strongly exothermic reaction coordinates toward IC. Moreover, the rates of IC were found to be independent of the protonation state of the protein. The theoretical studies[12−17] of the S_1 potential energy surface (PES) and the minimum energy conical intersection (MECI) points did not provide a simple unifying explanation; e.g., volume-conserving (i.e., hula-twist) pathways to MECI were found to have large barriers, whereas lower-energy relaxation coordinates correspond to nonvolume-conserving motions.

Properties of the gas phase chromophores of the GFP type have been considered in several theoretical studies (see the recent review[18]) using methods ranging from semiempirical models[19−24] to time-dependent density functional theory (TD-DFT)[10,21−23,25−31] and different *ab initio* approaches.[10,16,17,32−42] A majority of these papers focused on the absorption spectra of the chromophore (or its oxidized forms[44]) in the ground electronic state, and only a few works described the chromophore properties in the S_1 excited state. Calculations of Martin et al.[16] for the anionic form of HBDI performed using CASSCF(12/11)/6-31G* and CASPT2//CASSCF suggested an extremely flat landscape of the S_1 PES in the region of the potentially fluorescent state (called FS in ref 16). The details of the S_1 PES including the energy minima and the minimum energy conical intersection points were computed with the two-root (S_0, S_1) state-averaged (SA2-CASSCF) procedure with equal weights (w1 = 1, w2 = 1). The calculated S_0-S_1 energy gap at the FS point corresponded to the wavelength of 507 nm (2.45 eV).[16] The paper of Altoe at el.[17] mainly focused on the vibrational properties of the ground state anionic, neutral, and cationic forms of HBDI in solution but also included the results for the gas-phase photoreaction pathway of the HBDI anion. These calculations were carried out using the SA2-CASSCF(12,11)/6-31G* wave functions and single-state perturbation theory (CASPT2) corrections. In both papers,[16,17] a twisted type intersection between the S_1 and S_0 PESs was reported. Olsen and Smith[37] employed SA3-CASSCF(4/3)/DZP to compute stationary points on the S_0 and S_1 surfaces,

as well as to optimize the S_1/S_0 MECI. The energies at these points were recalculated with multireference multistate Rayleigh−Schrödinger perturbation theory (MR-MSRSPT2). The authors of ref 37 compared their conclusions to those reported previously by Martin et al.[16] and Altoe et al.[17] Simulations of photodynamics of the neutral form of HBI and HBDI in vacuo, in solution and in the protein, including calculations of the S_0 and S_1 energies and the MECI points performed by Martinez et al.[15,38] were based either on semiempirical or on the *ab initio* SA2-CASSCF(2,2)/6-31G methods.

A recent study[45] investigated the effect of protonation on the excited-state isomerization of isolated HBI by *ab initio* molecular dynamics with SA-CASSCF(2,2)/6-31G. The authors observed that both neutral (protonated) HBI and the anion forms undergo fast isomerization; however, the former species isomerizes exclusively around τ_I (the imidazolinone CC bond, see Figure 1a), whereas the latter species rotates mostly around the phenolate CC bond (τ_P), although the τ_I channel is also open. The difference was explained in terms of the effect of resonance on the bond alternation pattern in the two forms; i.e., protonation detunes the resonance in HBI. Owing to the well-known tendency of CASSCF to exaggerate bond alternation, the exact branching ratios (and the barriers) may be sensitive to the electronic structure methods employed. This study suggested that excited-state cis−trans isomerization may be strongly coupled with (gated by) protonation.[45]

For the purpose of our study, the results of Olsen and Smith[37] for the PES stationary points in the vicinity of the cis isomer (called Z isomer in ref 37) of the HBDI anion (Figure 1b) at the SA3-CASSCF(4/3)/DZP and the perturbatively corrected levels present the important reference data. We employ a similar strategy, namely, the state-averaged SA-CASSCF/cc-pVDZ and the state-specific CASSCF (w1 = 0, w2 = 1) approaches with a larger active space than that in ref 37 and the versions of the multiconfigurational quasi degenerate perturbation theory of the second order (MCQDPT2)[46,47] on top of SA-CASSCF to characterize all four protonation forms of HBDI in the S_1 state. For selected energy differences, we also report the EOM-CCSD/6-311G* and SOS-CIS(D)/cc-pVTZ values.

It is established that absorption in the protein occurs in the neutral and anionic protonation forms of the chromophore; but, the fluorescence is only due to the anionic form.[2] However, the involvement of the cationic and zwitterionic forms (Figure 1c,d) in the GFP photodynamics cannot be ruled out since the imidazolinone nitrogen may be protonated through a conservative Glu amino acid residue that is hydrogen bonded to the chromophore.[19]

The photocycle of the chromophore is initiated by the $\pi-\pi^*$ transition (i.e., $S_0 \rightarrow S_1$). The $S_1 \rightarrow S_0$ fluorescence may be observed from the presumably planar minimum on the S_1 PES. The radiationless relaxation from S_1 to S_0 is likely to proceed via conformational changes over the twisting angles τ_P and τ_I (Figure 1a). The same twisting motions lead to the sharp drop of the oscillator strength. Thus, even if the chromophore remains in the S_1 state at the twisted configuration, the fluorescence will be lost. The magnitudes of the barriers separating the planar minima in the vicinity of the Franck−Condon region from the twisted conformers and/or MECI points are crucial for understanding the excited-state lifetimes and fluorescent properties of the chromophore.

We report accurate calculations of the absorption and emission band maxima as well as locations of the MECI points and relevant energy barriers for all four protonated forms of HBDI. For the anionic form, our value of the absorption wavelength is close to the experimental gas phase values,[7,8,10] and the location of the MECI point is close to that obtained by Olsen and Smith.[37] This validates our results for the neutral, cationic, and zwitterionic forms.

These data are necessary to rationalize the properties of the GFP-type chromophores inside the protein by allowing one to separate the intrinsic properties of the chromophore from the role of the protein matrix. A direct comparison of geometry configurations and energies of the various critical points in the excited state in the gas phase and in the protein will help to elucidate the photochemical mechanism.

Methods

Geometry optimizations of the ground electronic states were performed using DFT (PBE0/cc-pVDZ) and RI-MP2/cc-pVTZ. The location of the minimum energy points and a partial scan of the S_1 PES were performed either using CASSCF/cc-pVDZ for the second root of the Hamiltonian or using state-averaged (SA) CASSCF. Energy differences between the S_0 and S_1 states at the selected geometries were computed with the perturbatively corrected CASSCF-based methods with the cc-pVDZ basis set as well as by SOS-CIS(D)/cc-pVTZ and EOM-EE-CCSD/6-311G* (the core electrons were frozen in the EOM calculations).

EOM-CC[48] and SOS-CIS(D)[49,50] calculations were performed using Q-Chem.[51] Multireference calculations were carried out with the Firefly computer program.[47] We employed two new procedures that are important for MECI point calculations, which were recently developed and implemented in Firefly: (I) analytic gradients for SA-CASSCF and (II) corrected MCQDPT2. The latter development corrected the bugs in the MCQDPT2 procedure,[46] resulting in a new version of the program called XMC-QDPT2. We refer to the Firefly Web site[47] for the technical details relevant to the calculations of MECI points and XMCQDPT2.

The calculations for each protonation form were initiated from the coordinates of the respective cis isomer. We then considered deformations over the angles τ_I and τ_P relaxing all other coordinates until the conical intersection or twisted minimum on S_1 was reached. We did not attempt to describe the photoinduced cis−trans isomerization of the chromophore.

Molecular Orbital Framework

Figure 2 illustrates relevant molecular orbitals (MOs) of different protonated forms of HBDI.

For all four forms, the excited S_1 state is derived from the HOMO to the valence LUMO transition (when using large bases, the valence LUMO may appear above a manifold of diffuse orbitals that fill the HOMO−LUMO gap). Both

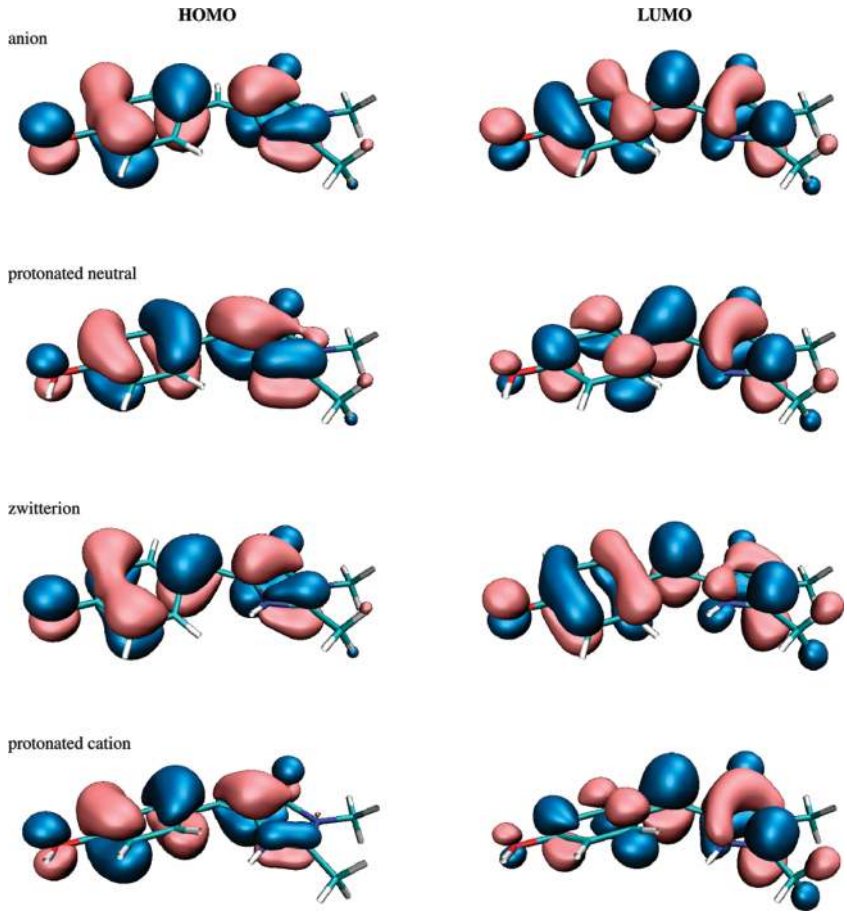

Figure 2. Frontier molecular orbitals of the anionic, neutral, zwitterionic, and cationic forms of HBDI, HOMO (left) and LUMO (right), computed by HF/6-311G*.

orbitals are of the π type and exhibit allylic character in the bridge region.[44] Despite the delocalized nature of the orbitals, the oscillator strength of S_1 and structural changes (e.g., in bond alternation and permanent dipole moment) induced by excitation can be explained by focusing on the bridge moiety (see refs 37, 39, 40, and 44).

The shapes of the MOs of the anionic and neutral HBDI are similar; however, the protonation stabilizes the HOMO considerably. For example, the vertical detachment energy (VDE) of the anionic form is 2.54 eV,[44] whereas the respective ionization energy for the neutral is 7.29 eV. Moreover, the protonation detunes the resonance. Consequently, instead of an almost perfectly allylic pair of orbitals in the anionic forms, the HOMO and LUMO in the neutral form develop π(C−C(I)) and π^*(C−C(I)) characters, respectively [C denotes the bridge carbon atom, and C(I) denotes an imidazolinone cycle carbon atom bonded directly to the bridge carbon]. This difference explains more pronounced bond alternation in the neutral form, in which the C−C(I) bond is much shorter than the C−C(P) one (see Table 1) [C(P) denotes the carbon atom of the phenolic ring bonded directly to the bridge carbon].

This difference in frontier orbitals also leads to larger changes in bond alternation in the S_1 state resulting in the sharper-shaped PES for the neutral form as compared to the extremely flat surface of the anionic form.

Stabilization of the HOMO in the protonated (neutral) form is responsible for a higher $S_0 \rightarrow S_1$ excitation energy (see below), which can be explained within the Hückel model. Alternatively, these changes in the electronic character of the bright state may be explained with the three-state valence-bond-like model.[37]

Table 1. Relevant Geometric Parameters of the Four Forms of HBDI Optimized with RI-MP2/cc-pVTZ[a]

	anion	neutral	zwitterion	cation
C(I)−C	1.378	1.350	1.395	1.350
C(P)−C	1.394	1.435	1.374	1.424
C=O (I)	1.233	1.216	1.222	1.201
C=O (P)	1.249	1.359	1.233	1.340
Twist	0	0	17.2	22.1

[a] Angles in degrees, bond lengths in Å.

The picture of MOs for the zwitterionic form is consistent with an inverted bond alternation pattern (see Table 1); namely, the HOMO and LUMO bear π(C−C(I)) and π^*(C−C(I)) characters, respectively. The structure and MOs of the protonated cationic form are similar to those of the neutral form.

Results for the Anionic Form

The cis-anionic form of the GFP chromophore (Figure 1b) is believed to be responsible for emission inside the protein matrix.[2] No fluorescence of the HBDI anion is detected in the gas phase due to rapid radiationless decay of the excited state population.[11] The position of the optical absorption band

Table 2. Calculated Vertical S_0-S_1 Excitation Energies of the Anionic (Deprotonated) Form of the GFP Chromophore[a]

system, calculation details	λ, nm	ΔE, eV	ref
HBI, CASPT2//CASSCF(12/11)/6-31G*	465	2.67	16
HBDI, CASPT2/cc-pVTZ//DFT(BLYP)[b]	431	2.88	41
HBDI, EOM-CCSD/cc-pVDZ//DFT(BLYP)	408	3.04	41
HBDI, EOM-CCSD/6-311G*//RI-MP2/cc-pVTZ	400	3.10 (1.25)	t.w.
HBDI, SOS-CIS(D)/cc-pVTZ//RI-MP2/cc-pVTZ	473	2.62 (1.54)	39
HBDI, XMCQDPT2/cc-pVDZ//DFT(PBE0)/cc-pVDZ	494	2.51 (1.19)	t.w.

[a] Oscillator strength is given in parentheses. The experimental gas phase value[5,6] is 2.59 eV or 479 nm. [b] CASPT2/cc-pVTZ//DFT(BLYP) calculations from ref 41 employed the default IPEA corrected zero-order Hamiltonian (the MOLCAS 7.2 program).

in the gas phase corresponding to the S_0-S_1 vertical excitation was measured by photodestruction spectroscopy of mass-selected ions injected into an electrostatic ion storage ring.[7,8] The band is centered at 479 nm (or 2.59 eV) extending from 2.4 to 2.8 eV (440−520 nm). Several theoretical papers reported fairly good results for this band either for the HBDI molecule or for a slightly simplified HBI model system by using different ab initio methods; however, the resonance (autoionizing) nature of this state[11,39] complicates the interpretation of the experimental spectrum and makes it difficult to obtain a converged theoretical value of the band maximum. Table 2 summarizes the majority of the previously published excitation energies for the vertical $S_0 \rightarrow S_1$ transition. The detailed discussion of the methods' performance can be found elsewhere;[39,41] we only note that the value computed in this work with XMCQDPT2/SA2-CASSCF(14/12)/cc-pVDZ//DFT(PBE0)/cc-pVDZ (494 nm or 2.51 eV) is within 15 nm (0.08 eV) from the experimental maximum at 479 nm (2.59 eV).[7,8]

It is important to compare our results for the selected critical points on the S_0 and S_1 PES to those obtained by Olsen and Smith.[37] Figure 3 presents the energy diagram for the anionic form of HBDI showing the energies at the ground state minimum (Min-S_0), at the planar minimum on the excited state (Plan-S_1), at the S_0/S_1 MECI point attainable by the τ_I twist (MECI−I-$S_{0/1}$), and at the twisted over angles τ_I and τ_P minimum energy points on the excited state (TwI-S_1 and TwP-S_1). Owing to the very flat shape of the S_1 PES, we were able to obtain only approximate values of the barriers on S_1.

The coordinates and the total energies of the critical points on the PESs calculated in this work using DFT(PBE0)/cc-pVDZ for S_0 and SA-CASSCF(12/11)/cc-pVDZ for S_1 are given in the Supporting Information. First, we note that the geometries computed in this work are consistent with those shown in Figure 8 and Figure 9 of ref 37. Table 3 presents the selected geometric parameters of the Min-S_0, Plan-S_1, TwI-S_1, and MECI−I-$S_{0/1}$ structures of the deprotonated HBDI anion. We observe significant elongation of the C(I)−C and C(P)−C bonds in the Plan-S_1 structure relative

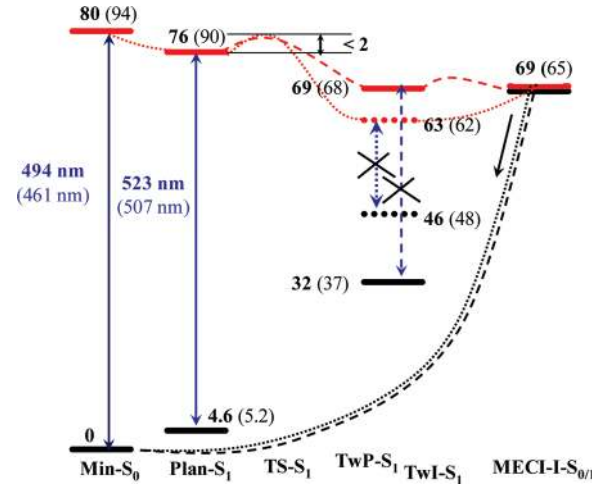

Figure 3. Energy diagram of the anionic (deprotonated) form of HBDI at the cis conformation (Figure 1b). Thick black horizontal lines denote the ground state (S_0) levels; thick red lines - the excited state (S_1) levels. The structures corresponding to the minimum on S_0 (Min-S_0), the planar minimum energy point on S_1 (Plan-S_1), the MECI point (MECI−I-$S_{0/1}$), and the minimum on S_1 twisted over τ_I (TwI-S_1) and τ_P (TwP-S_1) are indicated. The energy values (in kcal/mol) in parentheses refer to the data of Olsen and Smith obtained at the SA3-CASSCF(4,3)/DZP level.[37] The energy values in bold (in kcal/mol) refer to the present calculations with SA-CASSCF(12/11)/cc-pVDZ. The SA means equal weighting average over the first two states (w1 = 1, w2 = 1) for all of the structures when computing the S_0 and S_1 state energies. The TwP-S_1, TwI-S_1, and MECI structures were optimized using the SA procedure; the (0,1) weighting state-specific treatment was employed for locating the Plan-S_1 and TS-S_1 structures' location. We also show the wavelengths for the vertical transition energies corresponding to the S_0-S_1 gap at Min-S_0 and Plan-S_1 computed in this work (in bold) and previously[37] (in parentheses) by using the highest theoretical levels in both works: XMCQDPT2/CASSCF(14/12)/cc-pVDZ//DFT-(PBE0)/cc-pVDZ at Min-S_0; XMCQDPT2/CASSCF(14/12)/cc-pVDZ//SS-CASSCF(12/11)/cc-pVDZ at Plan-S_1; and MS-CASPT2//SA3-CASSCF(4,3)/DZP.[37]

Table 3. Selected Geometric Parameters of the HBDI Anion Optimized with CASSCF(12/11)/cc-pVDZ[a]

	Min-S_0	Plan-S_1	TwI-S_1	MECI−I-$S_{0/1}$
C(I)−C	1.376	1.423	1.461	1.468
C(P)−C	1.414	1.455	1.414	1.457
C=O (I)	1.213	1.222	1.209	1.192
C=O (P)	1.222	1.227	1.236	1.255
Twist-I	0	0	91.612	115.921
Twist-P	0	0	0.88	11.20

[a] Angles in degrees, bond lengths in Å. "Twist-I" is the N−C(I)−C−H dihedral angle value; "Twist-P" is the H−C−C(P)−C dihedral angle value.

to Min-S_0. This change is due to partial charge transfer from the C(I)−C and C(P)−C bonds (HOMO) to the CH bridge (LUMO) (see Figure 2 and the Supporting Information). The TwI-S_1 structure has an even longer C(I)−C distance because the N−C(I)−C−H dihedral angle is close to 90°, which disrupts the conjugation between the rings, thus making C(I)−C a single bond. The MECI−I-$S_{0/1}$ structure develops new features (as compared to TwI-S_1): notable are a Twist-P

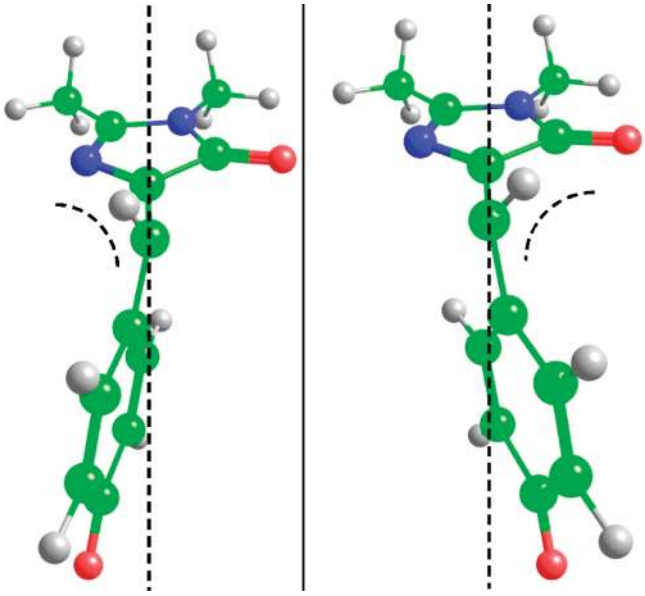

Figure 4. Two I-twisted MECI structures found in this work. The left one was obtained by starting from the trans structure, and the right one - from the cis structure.

angle value of ~10° and visible pyramidalization at the bridge carbon.

Our energy gaps also agree fairly well with those from ref 37 despite the differences in the calculation schemes (the size of the active space, the state-averaging procedure, and the treatment of perturbation corrections). The flat landscape of the S_1 PES along the τ_I angle shown in Figure 10 of ref 37 is consistent with an almost negligible barrier height (less than 2 kcal/mol) required to climb out of the planar S_1 minimum estimated in our work. Similar values of barrier heights on S_1 were reported in refs 16 and 17. For the I-Twist structure, we found two different MECI points depending on the starting point for optimization (either from the trans or cis structures). The difference between these MECI points, which is due to asymmetry of the imidazolinone ring, can easily be seen in Figure 4. The energy difference between these structures is less than 1 kcal/mol (see the Supporting Information). We were not able to locate the MECI-P structure—all of the searches eventually ended up at MECI-I.

The S_0-S_1 energy gap at Plan-S_1 computed in this work is 523 nm (2.37 eV), and this transition has a large oscillator strength. As expected from the MO shapes (see Figure S5 in the Supporting Information), the S_0-S_1 transitions at TwI-S_1 and TwP-S_1 are forbidden, as indicated by the crosses in Figure 3.

Overall, these results are consistent with the experimental findings;[7,8] namely, fluorescence from the anionic GFP chromophore in the gas phase is hardly possible since upon excitation the system can evolve almost freely on the S_1 surface toward optically dark structures and the conical intersection point (MECI−I-$S_{0/1}$). The dramatic change in fluorescence properties and excited state lifetime in the protein suggests that the protein environment strongly affects the shape of the S_1 PES, increasing the barriers along the twisting coordinate.

Results for the Neutral Form

The neutral form of the GFP chromophore (Figure 1a) is responsible for the shorter wavelength absorption at ~400 nm (3.10 eV), but not for steady-state emission inside the protein matrix.[2] Attempts to determine the gas phase absorption using the photodestruction spectroscopy through the positively charged model systems mimicking the true neutral chromophore are presented in refs 9 and 10. The most recent paper from the Andersen group[10] reports a revised value of the band maximum, which is closer to 370 nm (3.35 eV) rather than to 415 nm (2.99 eV) as claimed earlier.[9]

The wavelength of 370 nm (3.35 eV) is also consistent with the results of the most recent quantum chemical calculations.[10,24,41] It should be noted that neutral HBDI (or HBI) presents a difficult case for the CASSCF-based methods. Unlike the anionic form, the desired excited $\pi\pi^*$ state of the neutral does not appear as the second root of the CAS-CI Hamiltonian for various choices of the active space (up to the CASSCF(16/14) partitioning[35]) with different basis sets. Consequently, the state averaging should be performed for more than two states. In particular, Bravaya et al.[36] applied the SA4-CASSCF(16/14) method to optimize the orbitals and the expansion coefficients followed by aug-MCQDPT2[52] to compute the excitation energy at 3.11 eV (or 399 nm). Unfortunately, later, bugs in the original MCQDPT2 code were found,[47] and the predictions of these calculations should be revisited. In this work, we applied SA3-CASSCF(14/12)/cc-pVDZ followed by the XMC-QDPT2 method[47] to compute the S_0-S_1 energy gap at Min-S_0 (which in turn was optimized at the PBE0/cc-pVDZ level). The computed wavelength, 375 nm (3.31 eV), practically coincides with the most recent experimental measurement of 370 nm (3.35 eV).[10]

The EOM-CCSD and SOS-CIS(D) calculations yield considerably higher excitation energies, i.e., 3.83 and 4.12 eV, respectively. While there are discrepancies between the excitation energy values, all methods agree that the absorption of the protonated form is strongly blue-shifted (1.0−1.2 eV) relative to that of the anion. Table 4 summarizes the results of the excitation energy calculations.

The geometry of the planar minimum (Plan-S_1) in the S_1 state was optimized with the CASSCF(12/11)/cc-pVDZ method for the true second root (w1 = 0, w2 = 1). The S_1-S_0 energy gap at this point was calculated by using the XMCQDPT2/SA2(w1=1,w2=1)CASSCF(14/12) approach, that is, at the same level as for the anionic form. Thus, we report here an accurate theoretical estimate for the wavelength, 459 nm (2.70 eV), of the allowed $S_1 \rightarrow S_0$ transition of neutral HBDI in the gas phase. We were able to locate saddle points on the S_1 PES at the SA2-CASSCF(12/11)/cc-pVDZ level for the true second root (w1 = 0, w2 = 1). The first one corresponds to the twisting over angle τ_P with the only imaginary frequency of 64i; the second corresponds to the twisting over angle τ_I with the only imaginary frequency of 209i. Their energies are about 8−9 kcal/mol above those of Plan-S_1;

Table 4. Calculated Vertical S_0-S_1 Excitation Energies of the Neutral Form of the GFP Chromophore[a]

system, calculation details	λ, nm	ΔE, eV	ref
HBDI, CASPT2/cc-pVDZ// DFT(BLYP)[b]	346	3.58	41
HBDI, EOM-CCSD/cc-pVDZ// DFT(BLYP)	310	4.00	41
HBDI, R1-CC2/aug-cc-pVDZ// CC2/aug-cc-pVDZ	349	3.55	10
HBDI, aug-MCQDPT2/aug-cc-pVDZ//MP2/(aug)-cc-pVDZ	399	3.11	10, 36
HBDI, EOM-CCSD/6-311G*// RI-MP2/cc-pVTZ	301	4.12 (0.82)	this work
HBDI, SOS-CIS(D)/cc-pVTZ// RI-MP2/cc-pVTZ	324	3.83 (1.10)	this work
HBDI, XMCQDPT2/cc-pVDZ// DFT(PBE0)/cc-pVDZ	375	3.31 (0.51)	this work

[a] Oscillator strength is given in parentheses. The experimental gas-phase value[10] is 3.35 eV or 370 nm. [b] The CASPT2/cc-pVTZ// DFT(BLYP) calculation from ref 41 employed the default IPEA zero-order Hamiltonian (by using the MOLCAS 7.2 program).

therefore, the planar minimum on S_1 can, in principle, be populated in the gas phase, given that the excited-state proton transfer is less favorable in the absence of a hydrogen-bonding network.

The coordinates of the twisted minimum (TwI-S_1) and of the MECI point (MECI−I-$S_{1/0}$) were located at the SA2-(w1=1,w2=1)CASSCF(12/11) level. The S_1-S_0 transition from TwI-S_1 has negligible oscillator strength. The energy of the conical intersection point (MECI−I-$S_{0/1}$) is approximately equal to the energy of the planar minimum. The diagram in Figure 5 summarizes the results. Selected geometric parameters of the Min-S_0, Plan-S_1, TwI-S_1, and MECI−I-$S_{0/1}$ structures are collected in Table 5.

In the Plan-S_1 structure, the C(I)−C bond stretches by 0.077 Å due to redistribution of the electronic density in the bridge region in the excited state relative to the ground state. For the same reason, the C(P)−C bridge bond shortens by 0.042 Å. The change in other bond lengths is less pronounced, but still notable. The TwI-S_1 structure is similar to that of the anion with the Twist-I angle being close to 90° and Twist-P being close to 0°. MECI−I-$S_{0/1}$ differs from that of the anionic form: the Twist-P angle is closer to zero, and there is no visible pyramidalization at the bridge carbon; instead, this structure features pyramidalization at the C(I) carbon. The MECI-$S_{0/1}$ structure suggests that the decay to the ground state can lead to both isomers, cis and trans, with almost equal probabilities.

Results for the Cationic Form

Table 6 and the diagram in Figure 6 show the results for the cationic form (Figure 1c) using the same methodology as for the anionic and neutral forms. First of all, we note that the S_0-S_1 transition wavelength at the ground state minimum energy point computed with XMCQDPT2/SA2-CASSCF(14/12)/cc-pVDZ//DFT(PBE0)/cc-pVDZ equals 406 nm (3.05 eV), which coincides with the experimental value of 406 nm.[8,9]

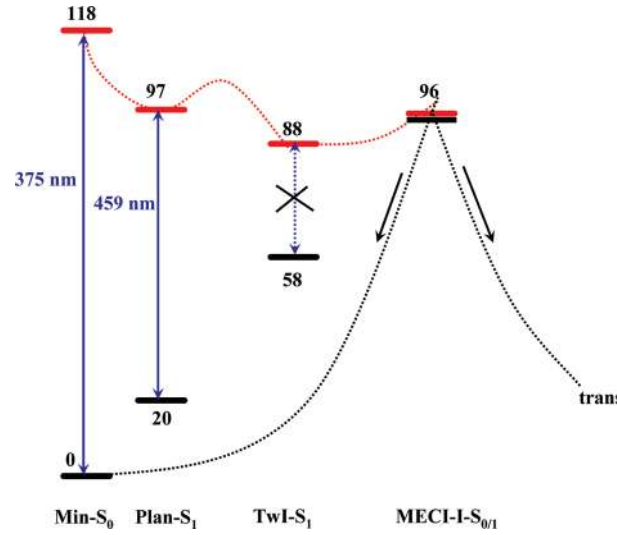

Figure 5. Energy diagram for the neutral form of HBDI in the vicinity of the cis conformation (Figure 1a). Thick black horizontal lines denote the ground state (S_0) levels; thick red lines - the excited state (S_1) levels. Structures corresponding to the minimum energy point on S_0 (Min-S_0), the planar minimum energy point on S_1 (Plan-S_1), the MECI point (MECI−I-$S_{0/1}$), and the minimum energy point on S_1 twisted over τ_I (TwI-S_1) are shown. The energy values (kcal/mol) refer to the present calculations using SA-CASSCF(12/11)/cc-pVDZ. The SA means equal weighting average over the first three states for Min-S_0, two states for TwI-S_1 and MECI, and the (0,1) weighting for Plan-S_1. We also show the wavelengths for the vertical S_0-S_1 transition energies at Min-S_0 and Plan-S_1 computed using the highest theoretical level: XMCQDPT2/SA3-CASSCF(14/12)/cc-pVDZ//DFT(PBE0)/cc-pVDZ at Min-S_0; XMCQDPT2/SA2-CASSCF(14/12)/cc-pVDZ//SA2-CASSCF(12/11)/cc-pVDZ at Plan-S_1.

Table 5. Selected Geometric Parameters of Neutral HBDI Optimized with CASSCF(12/11)/cc-pVDZ[a]

	Min-S_0	Plan-S_1	TwI-S_1	MECI−I-$S_{0/1}$
C(I)−C	1.351	1.428	1.440	1.428
C(P)−C	1.468	1.426	1.398	1.423
C=O (I)	1.197	1.211	1.237	1.222
C=O (P)	1.361	1.366	1.332	1.340
Twist-I	0	0	90.23	68.28
Twist-P	0	0	1.067	0.319

[a] Angles in degrees, bond lengths in Å. "Twist-I" is the N−C(I)−C−H dihedral angle value. "Twist-P" is the H−C−C(P)−C dihedral angle value.

Table 6. Calculated Vertical S_0-S_1 Excitation Energies of the Cationic Form of the GFP Chromophore[a]

system, calculation details	λ, nm	ΔE, eV
HBDI, EOM-CCSD/6-311G*// RI-MP2/cc-pVTZ	345	3.60
HBDI, SOS-CIS(D)/cc-pVTZ// RI-MP2/cc-pVTZ	380	3.27 (1.08)
HBDI, XMCQDPT2/cc-pVDZ// DFT(PBE0)/cc-pVDZ	406	3.06 (0.87)

[a] Oscillator strength is given in parentheses.

The selected geometric parameters of the Min-S_0, Plan-S_1, TwI-S_1, and MECI−I-$S_{0/1}$ structures are collected in Table 7.

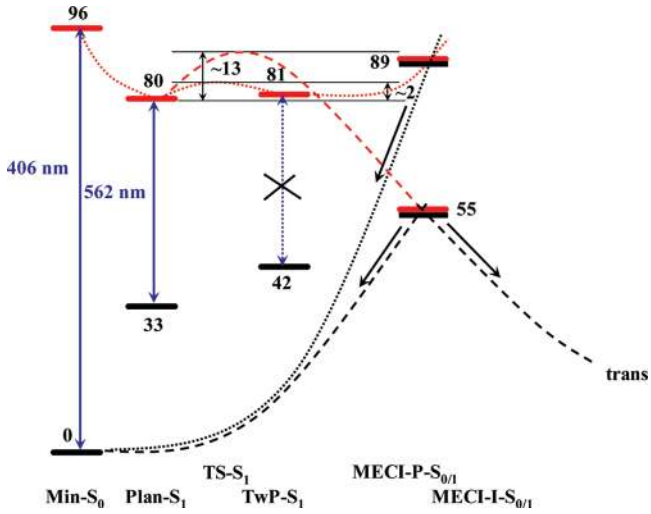

Figure 6. Energy diagram for the cationic form of HBDI at the cis conformation (Figure 1c). Thick black horizontal lines denote the ground state (S_0) levels; thick red lines - the excited state (S_1) levels. The structures corresponding to the minimum energy point on S_0 (Min-S_0), the planar minimum energy point on S_1 (Plan-S_1), the MECI points (MECI−P-$S_{0/1}$ and MECI−I-$S_{0/1}$), and the minimum energy point on S_1 twisted over τ_P (TwP-S_1) are shown. The energy values (kcal/mol) refer to the present calculations with SA2-CASSCF(12/11)/cc-pVDZ. The MECI structures were calculated with equal weighting average over the first two states, whereas structures of Plan-S_1, Tw−P-S_1, TS−P-S_1, and TS−I-S_1 were calculated with the (0,1) weighting. We also show the wavelengths for the vertical S_0−S_1 transition energies at Min-S_0 and Plan-S_1 computed using the highest theoretical level: XMCQDPT2/SA2-CASSCF(14/12)/cc-pVDZ//DFT(PBE0)/cc-pVDZ at Min-S_0; XMCQDPT2/SA2-CASSCF(14/12)/cc-pVDZ//SA2-CASSCF(12/11)/cc-pVDZ at Plan-S_1.

Table 7. Selected Geometric Parameters of the HBDI Cation Optimized with CASSCF(12/11)/cc-pVDZ[a]

	Min-S_0	Plan-S_1	MECI−I-$S_{0/1}$	MECI−P-$S_{0/1}$
C(I)−C	1.346	1.354	1.460	1.344
C(P)−C	1.470	1.453	1.389	1.473
C=O (I)	1.186	1.201	1.213	1.205
C=O (P)	1.341	1.300	1.313	1.264
Twist-I	5.32	2.99	86.90	3.17
Twist-P	32.768	8.378	2.313	82.36

[a] Angles in degrees, bond lengths in Å. "Twist-I" is the N−C(I)−C−H dihedral angle value. "Twist-P" is the H−C−C(P)−C dihedral angle value.

We also note that emission from the planar minimum on S_1 (Plan-S_1) corresponds to the wavelength of 562 nm (2.21 eV), which is the longest wavelength among various forms of HBDI. This planar minimum is separated from other stationary points on S_1 by the low-lying saddle point (less than 2 kcal/mol) with a single imaginary frequency of 92i. Another saddle point is more than 10 kcal/mol higher. There are two MECI points (MECI−P-$S_{0/1}$ and MECI−I-$S_{0/1}$) through which the decay to the ground state may occur. Emission from the twisted minimum on S_1, TwP-S_1, is forbidden.

The MECI−I-$S_{0/1}$ structure is similar to the TwI-S_1 structure of the anionic and neutral forms: Twist-I is close to 90°, whereas the Twist-P value is close to 0°. In MECI−P-$S_{0/1}$, the picture is reversed: Twist-P is close to 90°, and Twist-I is almost zero.

Table 8. Calculated Vertical S_0−S_1 Excitation Energies of the Zwitterionic Form of the GFP Chromophore[a]

system, calculation details	λ, nm	ΔE, eV
HBDI, EOM-CCSD/6-311G*// RI-MP2/cc-pVTZ	397	3.13 (1.09)
HBDI, SOS-CIS(D)/cc-pVTZ// RI-MP2/cc-pVTZ	477	2.60 (1.47)
HBDI, XMCQDPT2/cc-pVDZ// DFT(PBE0)/cc-pVDZ	503	2.46 (0.99)

[a] Oscillator strength is given in parentheses.

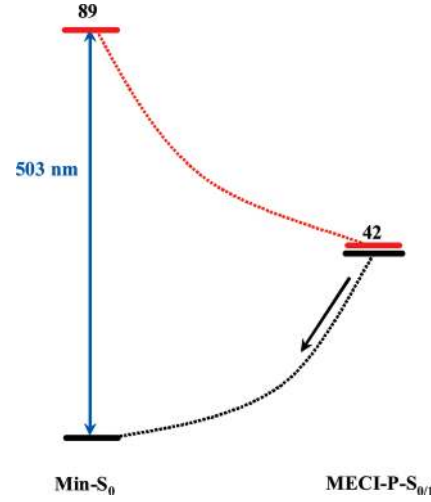

Figure 7. Energy diagram for the zwitterionic form of HBDI at the cis conformation (Figure 1d). Thick black horizontal lines denote the ground state (S_0) levels; thick red lines - the excited state (S_1) levels. The energy values (kcal/mol) refer to the present SA-CASSCF(12/11)/cc-pVDZ calculations. The SA means equal weighting average over the first two states (1,1). We also show the wavelength for the vertical $S_0 \rightarrow S_1$ transition at Min-S_0 computed with XMCQDPT2/CASSCF(14/12)/cc-pVDZ//DFT(PBE0)/cc-pVDZ.

Results for the Zwitterionic Form

The zwitterionic form of the GFP chromophore (Figure 1d) was considered in earlier studies[19] as a possible candidate for the emitting species. Our results are presented in Table 8 and in Figure 7.

Our calculations yield the simplest-shaped S_1 PES for this form, as shown in Figure 7. No minimum energy points on S_1 were located. Thus, the zwitterionic form would undergo barrierless relaxation to MECI, which is 47 kcal/mol below the Franck−Condon region. Zwitterionic MECI−P-$S_{0/1}$ resembles the structure of the anion's TwP-S_1: the Twist-P angle is almost 90°, the Twist-I is 0°, there is no pyramidalization at the bridge atoms, and C(I)−C is close to a double bond (1.36 Å as compared to 1.42 Å in Min-S_0), whereas C(P)−C stretches by 0.12 Å (see Table 9).

Results for the S_1−S_0 and S_0−S_1 Optical Transitions

The S_1−S_0 transition energies and oscillator strengths were calculated for the anionic, neutral, and cationic forms of

Table 9. Selected Geometric Parameters of the HBDI Zwitterion Optimized with CASSCF(12/11)/cc-pVDZ[a]

	Min-S_0	MECI−P-$S_{0/1}$
C(I)−C	1.420	1.363
C(P)−C	1.358	1.476
C═O (I)	1.214	1.204
C═O (P)	1.217	1.235
Twist-I	10.93	0
Twist-P	5.23	89.97

[a] Angles in degrees, bond lengths in Å. "Twist-I" is the N−C(I)−C−H dihedral angle value. "Twist-P" is the H−C−C(P)−C dihedral angle value.

HBDI at the Plan-S_1 geometry configurations (Table 10). For the zwitterionic form, the Plan-S_1 structure was not found, as described above.

The Stokes shift increases in a series: anion < neutral < cation. The shift for the anionic form in the gas phase (29 nm) is very close to the protein value of 32 nm.[1,2] Such a small value is due to strong resonance effects in the ground and excited states resulting in small geometry distortions of the respective equilibrium geometries (Min-S_0 and Plan-S_1). In the neutral form, the resonance is partially broken, and the structural differences are more pronounced. The largest shift (156 nm) is observed for the cationic form and can be attributed to significant differences between the Min-S_0 and Plan-S_1 structures described above. We note that the cationic structure shows not only the largest Stokes shift but also the longest S_1-S_0 transition wavelength, which is red-shifted by 39 nm relative to the anion.

Reference 43 reported the energies of the bright S_0-S_1 transitions obtained with the SA-CASSCF, CASPT2/SA-CASSCF, TDDFT, and EOM-CC methods employing different basis sets. Table 11 compares our XMCQDPT2/SA-CASSCF(14/12)/cc-pVDZ results with the CASPT2/SA-CASSCF(2/2)/6-31G* values from ref 43.

The results for the anionic form agree well, whereas for other forms the differences are significant. The discrepanices can be explained by the features of configurational composition of the S_1 CASSCF bright states of these forms. The anionic wave function is dominated by the HOMO−LUMO transition, whereas for other protonated forms several other important configurations appear with considerable weights, which is not adequately accounted for in small active spaces.

Conclusions

We presented the results of quantum chemical calculations of the transition energies, equilibrium geometries, and conical intersection points for the first two singlet electronic states of the model GFP chromophore, HBDI, in the vicinity of its cis conformation in the gas phase. We described all four possible protonation states of the chromophore at the uniform level of theory. The anionic form has been studied in detail before;[16,17,37] however, the high-level results for other forms are reported for the first time. We note a very good agreement of our results with the experimental data for the absorption band wavelengths of the anionic, cationic, and neutral forms.

Table 11. Comparison of the Present and Previously Reported Computed Excitation Energies for the S_0-S_1 Transition of Different Protonated Forms of HBDI

	this work		ref 43	
system	λ, nm	ΔE, eV	λ, nm	ΔE, eV
HBDI, anion	494	2.51	490	2.53
HBDI, neutral	375	3.31	340	3.65
HBDI, cation	406	3.06	435	2.85
HBDI, zwitterion	503	2.46	440	2.82

The principal difference between the (deprotonated) anionic and neutral forms stems from the changes in the frontier MOs: the protonation detunes the resonance and breaks the almost perfectly allylic character of the anionic MOs. Consequently, the bond alternation in the ground state and its change in S_1 are more pronounced in the neutral.

The flat shape of the S_1 PES of the anionic chromophore found in our and previous calculations is consistent with the experimentally observed lack of fluorescence in the gas phase. Given the shape of the surface, the excited state should rapidly decay to twisted conformations thus preventing fluorescence from the Plan-S_1 structure. Apparently, the shape of the S_1 PES should be considerably different in the protein environment.

In contrast, in the neutral form, the planar minimum on the S_1 surface may, in principle, be populated in the gas phase. Fluorescence decay in this case would involve the I-twist motion with a notable barrier (~8 kcal/mol), and therefore, a longer lifetime is expected relative to the anion. The zwitterionic form has no planar minimum on the S_1 PES and features a low-lying MECI, thus enabling an efficient S_1 decay pathway through a space-conserving P-twist. The cationic S_1 surface turns out to be very flat along the P-twist coordinate featuring the P-twist minimum with a negligible S_1-S_0 oscillator strength. On the contrary, the barrier for I-twist is more than 13 kcal/mol, which is the largest value in our calculations. However, there is the I-twisted MECI point at lower energy relative to the plan-S_1 structure, so we cannot rule out this radiationless decay pathway. We also

Table 10. Calculated Vertical S_0-S_1 and S_1-S_0 Energies and the Respective Adiabatic Values of the Different Protonated Forms of the GFP Chromophore[a]

	S_0-S_1		S_1-S_0		
system and calculation details	λ, nm	ΔE, eV	λ, nm	ΔE, eV	Stokes shift, nm
HBDI, anion XMCQDPT2/SA2-CASSCF(14/12)/cc-pVDZ//CASSCF(12/11)/cc-pVDZ	494 (1.19)	2.51	523 (1.08)	2.37	29
HBDI, neutral XMCQDPT2/SA2-CASSCF(14/12)/cc-pVDZ//CASSCF(12/11)/cc-pVDZ	375 (0.51)	3.31	459 (0.36)	2.70	84
HBDI, cation XMCQDPT2/SA2-CASSCF(14/12)/cc-pVDZ//CASSCF(12/11)/cc-pVDZ	406 (0.87)	3.06	562 (0.44)	2.21	156

[a] Oscillator strength is given in parentheses.

note an enormous Stokes shift for the cationic form (156 nm) due to significant geometry relaxation in the Plan-S_1 state.

The I-twist energy profiles and the MECI structures suggest different excited-state isomerization pathways depending on the protonation state of the chromophore. The barrier for the I-twist motion decreases in the series: cation (13 kcal/mol) > neutral (8 kcal/mol) > anion (>2 kcal/mol). In the zwitterionic form, there is no Plan-S_1 stationary point, and a P-twist deactivation pathway is barrierless. The above barriers suggest that the motion along the I coordinate leading to twisted structures (minima and MECI) occurs much faster in the anionic form than in the neutral and cationic species. The gap between S_0 and S_1 at the Tw−I-S_1 geometry is 17 and 30 kcal/mol for the anionic and the neutral forms, respectively. With such small values (especially, 17 kcal/mol), one can expect a sufficient overlap between the S_0 and S_1 vibrational levels facilitating radiationless S_1-S_0 transition. Moreover, the SA-CASSCF calculations most likely overestimate the energy gap.[37] Overall, this result is in agreement with the observed ultrafast decay. Another pathway for the radiationless decay of the anionic form is via MECI, which is located almost at the same energy as Tw−I-S_1 but has a slightly different structure. Whereas the geometry of Tw−I-S_1 does not favor cis to trans isomerization over the return to the planar cis configuration on S_0, the MECI-I structure favors relaxation to the cis structure. In the neutral form, the MECI-I point is 8 kcal/mol above the Tw−I-S_1 structure. Both structures do not favor the relaxation to the cis structure over the isomerization. In the cationic form, MECI-I is the only twisted "minimum" on the S_1 surface along the I twist coordinate.

To summarize, the motion along the I coordinate for the anionic form is expected to be fast and may lead to cis to trans isomerization (with small yield) following S_1-S_0 radiationless transition via MECI-I. For the neutral and cationic forms, the relaxation should be slower due to larger energy gaps, and the structures do not favor any specific pathway, e.g., cis to trans isomerization versus the return the initial Plan-S_0 structure. Thus, we expect the isomerization yield to be higher for the neutral and cationic forms than for the anion. The I-Twisted conical intersections of the anionic, neutral, and cationic forms of the chromophore suggest possible pathways for the cis−trans isomerization, which is relevant to photoinduced dynamics in photoswitchable proteins.

Acknowledgment. This work was conducted under the auspices of the iOpenShell Center for Computational Studies of Electronic Structure and Spectroscopy of Open-Shell and Electronically Excited Species (http://iopenshell.usc.edu) supported by the National Science Foundation through the CRIF:CRF CHE-0625419 + 0624602 + 0625237 grant, as well as through the CHE-0951634 grant (A.I.K.). We thank Alex Granovsky and Dr. Ksenia Bravaya for generous help and valuable discussions. This work is also supported by the joint grant from the U.S. Civilian Research and Development Foundation (project RUC1-2914-MO-07) and the Russian Foundation for Basic Research (10-03-00085). I.V.P., B.L.G., and A.V.N. thank the SKIF-GRID program for providing resources at the SKIF-MSU, SKIF-SIBERIA, and UGATU computational facilities.

Supporting Information Available: Figures of the HBDI anion SA2-CASSCF(14/12)/cc-pVDZ, HBDI neutral SA3-CASSCF(14/12)/cc-pVDZ, HBDI zwitterion SA3-CASSCF(14/12)/cc-pVDZ, and HBDI cation SA3-CASSCF(14/12)/cc-pVDZ natural orbitals and their occupancies and the HBDI anion I-twisted minimum HOMO and LUMO orbitals. Tables of Cartesian coordinates. Details for the neutrals form S_0-S_1 transition XMCQDPT/CASSCF calculation. This material is available free of charge via the Internet at http://pubs.acs.org.

References

(1) Tsien, R. Y. *Annu. Rev. Biochem.* **1998**, *67*, 509.

(2) Zimmer, M. *Chem. Rev.* **2002**, *102*, 759.

(3) Nienhaus, G. U. *Angew. Chem., Int. Ed.* **2008**, *47*, 8992.

(4) Tonge, P. J.; Meech, S. R. *J. Photochem. Photobiol. A: Chem.* **2009**, *205*, 1.

(5) Meech, S. R. *Chem. Soc. Rev.* **2009**, *38*, 2922.

(6) van Thor, J. J.; Gensch, T.; Hellingwerf, K. J.; Johnson, L. N. *Nat. Struct. Biol.* **2002**, *9*, 37.

(7) Nielsen, S. B.; Lapierre, A.; Andersen, J. U.; Pedersen, U. V.; Tomita, S.; Andersen, L. H. *Phys. Rev. Lett.* **2001**, *87*, 228102.

(8) Andersen, L. H.; Lappierre, A.; Nielsen, S. B.; Nielsen, I. B.; Pedersen, S. U.; Pedersen, U. V.; Tomita, S. *Eur. Phys. J. D* **2002**, *20*, 597.

(9) Lammich, L.; Petersen, M. A.; Nielsen, M. B.; Andersen, L. H. *Biophys. J.* **2007**, *92*, 201.

(10) Rajput, J.; Rahbek, D. B.; Andersen, L. H.; Rocha-Rinza, T.; Christiansen, O.; Bravaya, K. B.; Erokhin, A. V.; Bochenkova, A. V.; Solntsev, K. M.; Dong, J.; Kowalik, J.; Tolbert, L. M.; Petersen, M. A.; Nielsen, M. B. *Phys. Chem. Chem. Phys.* **2009**, *11*, 9996.

(11) Forbes, M. W.; Jockusch, R. A. *J. Am. Chem. Soc.* **2009**, *131* (47), 17038.

(12) Olsen, S.; Manohar, L.; Martinez, T. J. *Biophys. J.* **2002**, *82*, 359.

(13) Toniolo, A.; Granucci, G.; Martinez, T. J. *J. Phys. Chem. A* **2003**, *107*, 3822.

(14) Megley, C. M.; Dickson, L. A.; Maddalo, S. L.; Chandler, G. J.; Zimmer, M. *J. Phys. Chem. B* **2009**, *113*, 302.

(15) Toniolo, A.; Olsen, S.; Manohar, L.; Martinez, T. J. *Faraday Discuss.* **2004**, *129*, 149.

(16) Martin, M. E.; Negri, F.; Olivucci, M. *J. Am. Chem. Soc.* **2004**, *126*, 5452.

(17) Altoe, P.; Bernardi, F.; Garavelli, M.; Orlandi, G.; Negri, F. *J. Am. Chem. Soc.* **2005**, *127*, 3952.

(18) Nemukhin, A. V.; Grigorenko, B. L.; Savitsky, A. P. *Acta Natur.* **2009**, *2*, 25.

(19) Voityuk, A. A.; Michel-Beyerle, M. E.; Rösch, N. *Chem. Phys. Lett.* **1997**, *272*, 162.

(20) Weber, W.; Helms, V.; McCammon, J. A.; Langhoff, P. W. *Proc. Natl. Acad. Sci. U.S.A.* **1999**, *96*, 6177.

(21) Gross, L. A.; Baird, G. S.; Hoffman, R. C.; Baldridge, K. K.; Tsien, R. Y. *Proc. Natl. Acad. Sci. U.S.A.* **2000**, *97*, 11990.

(22) Schäfer, L. V.; Groenhof, G.; Klingen, A. R.; Ullmann, G. M.; Boggio-Pasqua, M.; Robb, M. A.; Grubmüller, H. *Angew. Chem., Int. Ed.* **2007**, *46*, 530.

(23) Wan, S.; Liu, S.; Zhao, G.; Chen, M.; Han, K.; Sun, M. *Biophys. Chem.* **2007**, *129*, 218.

(24) Topol, I.; Collins, J.; Polyakov, I.; Grigorenko, B.; Nemukhin, A. *Biophys. Chem.* **2009**, *145*, 1.

(25) Marques, M. A. L.; Lopez, X.; Varsano, D.; Castro, A.; Rubio, A. *Phys. Rev. Lett.* **2003**, *90*, 258101.

(26) Lopez, X.; Marques, M. A. L.; Castro, A.; Rubio, A. *J. Am. Chem. Soc.* **2005**, *127*, 12329.

(27) Xie, D.; Zeng, X. *J. Comput. Chem.* **2005**, *26*, 1487.

(28) Nemukhin, A. V.; Topol, I. A.; Burt, S. K. *J. Chem. Theory Comput.* **2006**, *2*, 292.

(29) Sun, M. *Int. J. Quantum Chem.* **2006**, *106*, 1020.

(30) Amat, P.; Granucci, G.; Buda, F.; Persico, M.; Tozzini, V. *J. Phys. Chem. B* **2006**, *110*, 9348.

(31) Timerghazin, Q. K.; Carlson, H. J.; Liang, C.; Campbell, R. E.; Brown, A. *J. Phys. Chem. B* **2008**, *112*, 2533.

(32) Helms, V.; Winstead, C.; Langhoff, P. W. *THEOCHEM* **2000**, *506*, 179.

(33) Das, A. K.; Hasegawa, J.-Y.; Miyahara, T.; Ehara, M.; Nakatsuji, H. *J. Comput. Chem.* **2003**, *24*, 1421.

(34) Olsen, S.; Smith, S. C. *J. Am. Chem. Soc.* **2007**, *129*, 2054.

(35) Bravaya, K. B.; Bochenkova, A. V.; Granovsky, A. A.; Nemukhin, A. V. *Russ. J. Phys. Chem. B* **2008**, *2*, 671.

(36) Bravaya, K. B.; Bochenkova, A. V.; Granovsky, A. A.; Savitsky, A. P.; Nemukhin, A. V. *J. Phys. Chem. A* **2008**, *112*, 8804.

(37) Olsen, S.; Smith, S. C. *J. Am. Chem. Soc.* **2008**, *130*, 8677.

(38) Virshup, A. M.; Punwong, C.; Pogorelov, T. V.; Lindquist, B. E.; Ko, C.; Martínez, T. D. *J. Phys. Chem. B* **2009**, *113*, 3280.

(39) Epifanovsky, E.; Polyakov, I.; Grigorenko, B.; Nemukhin, A.; Krylov, A. I. *J. Chem. Theory Comput.* **2009**, *5*, 1895.

(40) Polyakov, I.; Epifanovsky, E.; Grigorenko, B.; Krylov, A. I.; Nemukhin, A. *J. Chem. Theory Comput.* **2009**, *5*, 1907.

(41) Filippi, C.; Zaccheddu, M.; Buda, F. *J. Chem. Theory Comput.* **2009**, *5*, 2047.

(42) Ma, Y.; Rohlfing, M.; Molteni, C. *J. Chem. Theory Comput.* **2010**, *6*, 257.

(43) Olsen, S. The electronic excited states of green fluorescent protein chromophore models, 2004. Stanford University Web Site. http://mtzweb.stanford.edu/resources/theses/olsen/olsenthesis.htm (accessed July 5, 2010).

(44) Epifanovsky, E.; Polyakov, I.; Grigorenko, B.; Nemukhin, A.; Krylov, A. *J. Chem. Phys.* **2010**, *132*, 115104.

(45) Olsen, S.; Lamothe, K.; Martínez, T. D. *J. Am. Chem. Soc.* **2010**, *132*, 1192.

(46) Nakano, H. *J. Chem. Phys.* **1993**, *99*, 7983.

(47) Granovsky, A. A. Firefly (former PC GAMESS) Home Page. http://classic.chem.msu.su (accessed July 5, 2010).

(48) Krylov, A. I. *Annu. Rev. Phys. Chem.* **2008**, *59*, 433.

(49) Grimme, S. *J. Chem. Phys.* **2003**, *118*, 9095.

(50) Rhee, Y. M.; Head-Gordon, M. *J. Phys. Chem. A* **2007**, *111*, 5314.

(51) Shao, Y.; Molnar, L. F.; Jung, Y.; Kussmann, J.; Ochsenfeld, C.; Brown, S.; Gilbert, A. T. B.; Slipchenko, L. V.; Levchenko, S. V.; O'Neil, D. P.; Distasio, R. A., Jr.; Lochan, R. C.; Wang, T.; Beran, G. J. O.; Besley, N. A.; Herbert, J. M.; Lin, C. Y.; Van Voorhis, T.; Chien, S. H.; Sodt, A.; Steele, R. P.; Rassolov, V. A.; Maslen, P.; Korambath, P. P.; Adamson, R. D.; Austin, B.; Baker, J.; Bird, E. F. C.; Daschel, H.; Doerksen, R. J.; Drew, A.; Dunietz, B. D.; Dutoi, A. D.; Furlani, T. R.; Gwaltney, S. R.; Heyden, A.; Hirata, S.; Hsu, C.-P.; Kedziora, G. S.; Khalliulin, R. Z.; Klunziger, P.; Lee, A. M.; Liang, W. Z.; Lotan, I.; Nair, N.; Peters, B.; Proynov, E. I.; Pieniazek, P. A.; Rhee, Y. M.; Ritchie, J.; Rosta, E.; Sherrill, C. D.; Simmonett, A. C.; Subotnik, J. E.; Woodcock III, H. L.; Zhang, W.; Bell, A. T.; Chakraborty, A. K.; Chipman, D. M.; Keil, F. J.; Warshel, A.; Herhe, W. J.; Schaefer III, H. F.; Kong, J.; Krylov, A. I.; Gill, P. M. W.; Head-Gordon, M. *Phys. Chem. Chem. Phys.* **2006**, *8*, 3172.

(52) Bravaya, K.; Bochenkova, A.; Granovsky, A.; Nemukhin, A. *J. Am. Chem. Soc.* **2007**, *129*, 13035–13042.

CT100227K